16th World Conference on Earthquake, 16WCEE 2017
Santiago Chile, January 9th to 13th 2017
Paper N° 3838
Registration Code: S- P1461954295

# SEISMIC PERFORMANCE EVALUATION OF FRENCH CREEK BRIDGE BASED ON CANADIAN HIGHWAY BRIDGE DESIGN CODE 2015

X. Li(1), Y. Kaya(2), C.E. Ventura(3)

*(1) Graduate Research Assistant, University of British Columbia, lxmichael52@gmail.com*
*(2) Research and Development Engineer, University of British Columbia, kayaya@mail.ubc.ca*
*(3) Professor, University of British Columbia, ventura@civil.ubc.ca*

## Abstract

Built in 1993, the French Creek Bridge is located near Parksville on Vancouver Island, British Columbia (BC), Canada. The bridge is part of the British Columbia Smart Infrastructure Monitoring System (BCSIMS), which is a real-time seismic monitoring program for bridges in BC. An ambient vibration test was conducted on the bridge in 2014 in order both to calculate the operational dynamic characteristics of the bridge and calibrate/update the finite element model of the bridge. The updated finite element of the bridge is then used to perform linear and nonlinear time history analysis, and push over analysis. Results obtained are used to determine the performance levels of the bridge in accordance with the Canadian Highway Bridge Design Code 2015. Results show that no primary members are expected to be damaged, and that the bridge will maintain repairable and operational during major earthquake.

*Keywords: Ambient Vibration Test, Model updating, Nonlinear dynamic analysis*

## 1. Introduction

In the late 1990's, a program called the British Columbia Smart Infrastructure Monitoring System (BCSIMS) was established by cooperation of Ministry of Transportation and Infrastructure (MoTI) BC and the Earthquake Engineering Research Facility (EERF) at the University of British Columbia (UBC), aiming at better preparation for possible seismic events and minimizing the damage of provincial Disaster Response Routes of BC [1]. One of the main purposes of the program is to establish a real-time seismic structural response system to provide instant inspection and rapid damage assessment for the Ministry's structures. The French Creek Bridge (FCB) was designed in 1993 and opened to traffic in 1996. The bridge is instrumented with 12 channels of acceleration sensors on and off the bridge.

As part of the BCSIMS project, an Ambient Vibration Test (AVT) was conducted in 2014. The data acquired in the AVT is used to extract the operational dynamic characteristics (e.g., natural frequencies, damping ratios, and mode shapes) of the bridge. Commercially available software, ARTeMIS® [2] is utilized to carry out the data processing and modal identification. The Finite Element (FE) model of the bridge is developed in CSibridge® and SAP2000® [3, 4]. The FE model is calibrated/updated based on the results obtained from the AVT. The updated model is then used to assess the seismic performance of the bridge in accordance with the Canadian highway bridge design code 2015 (CAN/CSA-S6-14) [5]. The updated FE model is used to perform linear and non-linear time history analysis, and push over analysis to determine the performance of each structural component. Results show that during major earthquake, no primary members (columns, cap-beams and girders) will be damaged, and that the bridge will maintain repairable and operational and should be capable of carrying the dead load plus full live load after major earthquake. There is, on the other hand, a high possibility that severe damage will happen at all bearings as well as the structural members that were connected to them.

## 2. Description of the French Creek Bridge (FCB)

As shown in Fig. 1, the French Creek Bridge is 212 meters long, 24.2 meters width with four vehicle lanes and two pedestrian lanes. Slope of the bridge floor is 1.6% that makes the elevation descents from south abutment to north abutment. The bridge is composed of five spans and is supported by three piers in the middle, one abutment at each end of the bridge, and one pile bent 10 meters away from the south end. Column heights of three piers are 26.9m, 26.8m and 21.6m respectively, the diameter of all pier columns is 2.44m. The superstructure of the bridge is composed of reinforced concrete deck casted on six W-shaped steel girders which develop throughout the bridge span (Fig.2). All girders are supported by fixed bearings and expansion bearings. The fixed bearings are located at three piers in the middle, and the expansion bearings are located at the south pile bent and north abutment. There are three expansion joints that divide the deck slab into four parts, and they are located at the south pile bent, the north abutment, and the pier No.3. Each pier is composed of two identical columns and a cap beam, which is connected to the bottom of steel girders via fix bearings. At each pier, both columns are supported by twenty-odd pipe piles being driven into the ground, all piles are driven into the bedrock beneath the foundation soil.

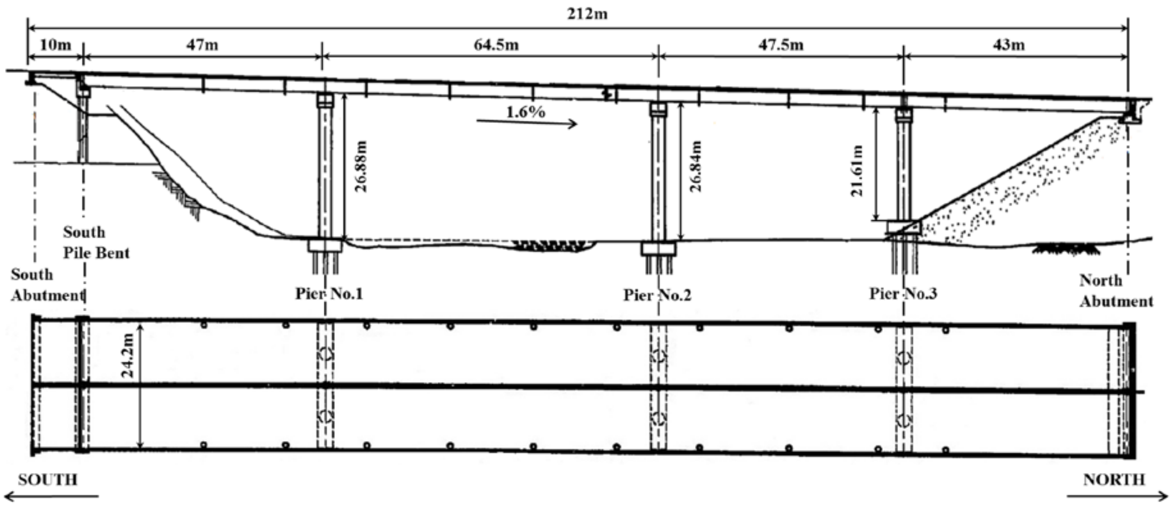


Fig. 1 – Elevation (top) and plan (bottom) view of the French Creek Bridge

Fig. 2 – Side view of concrete deck-steel girder system (left) and piers in middle spans (right)

## 3. Ambient Vibration Test (AVT) and Finite Element (FE) Model Updating/Calibration

Using the TROMINO® [6] sensors, an AVT test is carried out on the bridge in September, 2014 to calculate the modal properties (e.g., modal frequency, damping ratio, and mode shape) of the bridge. Eight TROMINO sensors were utilized in seven setups (Fig. 3). Sensor No.1 is selected as reference sensor and was placed at the middle span of southbound between pier 1 and 2 as shown in Fig.3. All of the sensors are oriented to the north end of the bridge, and one sensor is placed at each side of the expansion joints. The acquisition length for each setup is 30 minutes with sampling frequency of 128 Hz.

The Enhanced Frequency Domain Decomposition (EFDD) [7] techniques are used to identify the modal properties of the bridge. Peak-picking method was performed in order to identify the structural modes. The identified eight modes are summarized in Fig. 5.

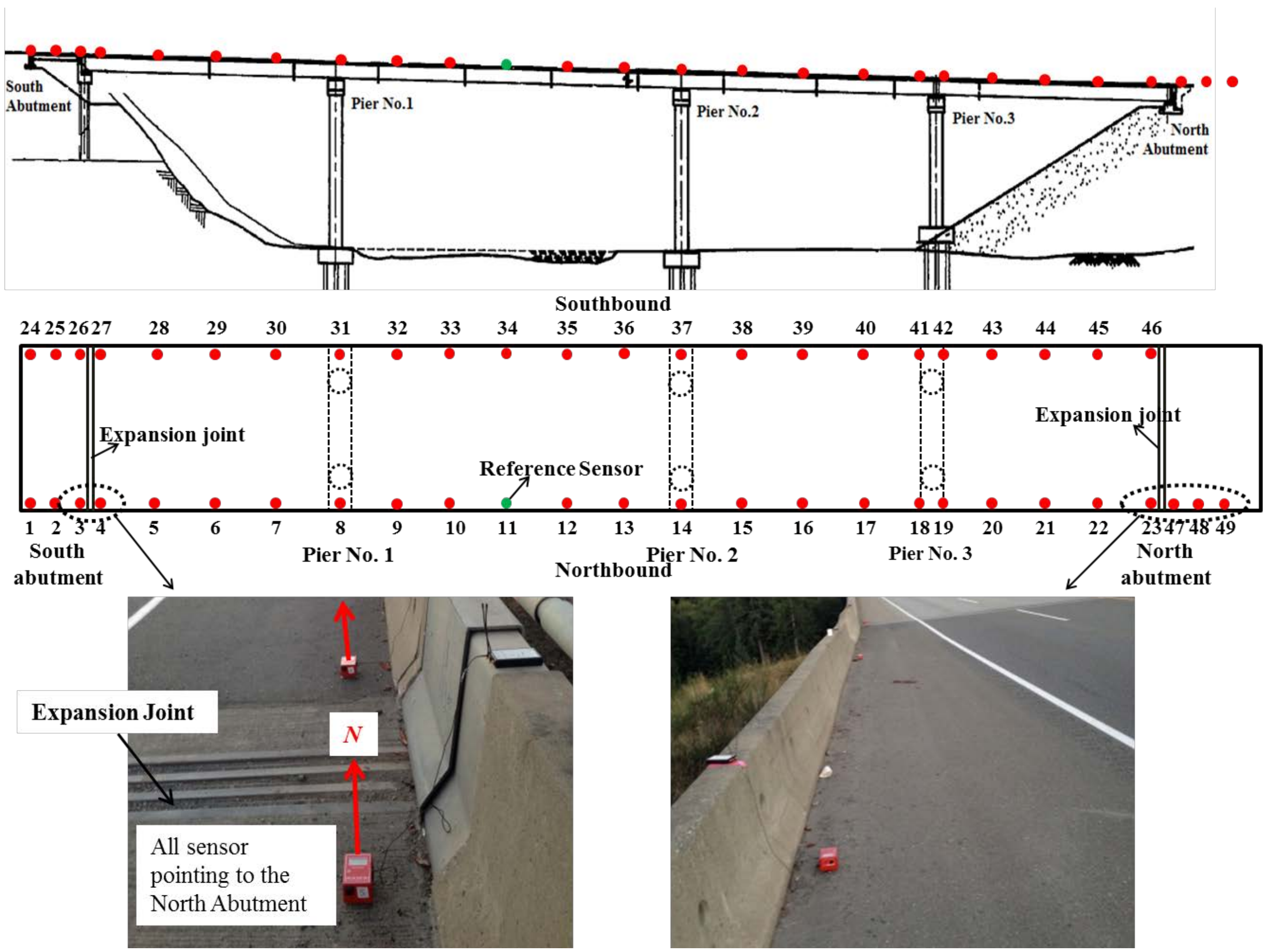


Fig. 3 – Setup plans and sensor locations of all setups

A FE model of the bridge is built in commercially available software SAP2000 (Fig.4). The major components of the bridge including superstructure, bearings, abutments, bents, piers and piles are modeled using frame, shell, and link elements. The natural frequencies and corresponding mode shapes of the bridge are calculated by Eigen analysis, and the updated modal frequencies and mode shapes are presented in Fig.5 along with the estimated modal parameters via the AVT for comparison.

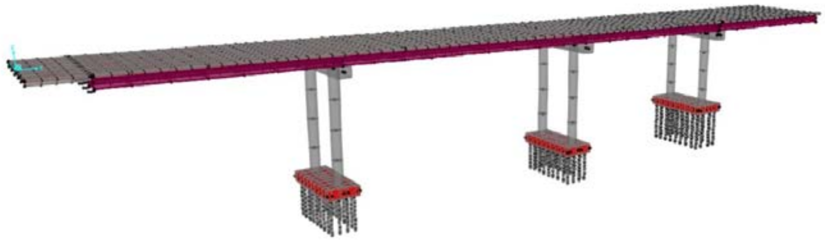

Fig. 4 – Overview of the Finite Element model of French Creek Bridge (SAP2000)

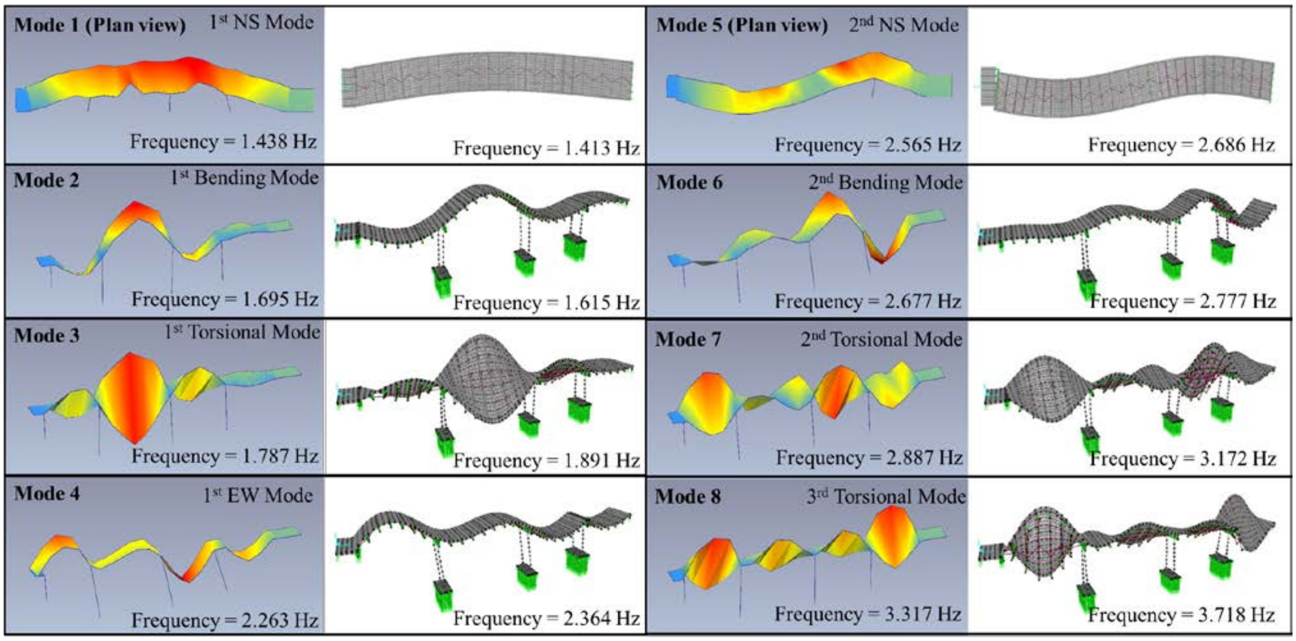


Fig. 5 – Comparison of the modal frequency and mode shapes of the bridge: AVT (left) and FE model (right)

Table 1 Natural frequencies before and after updating

| **Mode** | **Experimental frequency/Hz** | **$f_{FEA}$/Hz (before)** | **Error/%** | **$f_{FEA}$ /Hz (after)** | **Error/%** | **Frequency changed/%** |
|---|---|---|---|---|---|---|
| 1 | 1.438 | 1.176 | -22.28 | 1.413 | -1.77 | 20.15 |
| 2 | 1.695 | 1.592 | -6.47 | 1.615 | -4.95 | 1.44 |
| 3 | 1.787 | 1.852 | 3.51 | 1.891 | 5.50 | 2.11 |
| 4 | 2.263 | 1.916 | -18.11 | 2.364 | 4.27 | 23.38 |
| 5 | 2.565 | 2.332 | -9.99 | 2.686 | 4.50 | 15.18 |
| 6 | 2.677 | 2.634 | -1.63 | 2.777 | 3.60 | 5.43 |
| 7 | 2.887 | 2.950 | 2.14 | 3.172 | 8.98 | 7.53 |
| 8 | 3.317 | 3.219 | -3.04 | 3.718 | 10.79 | 15.50 |

As shown in Table 1, although the calculated mode shapes of the SAP2000 are very consistent with that of identified from the AVT, significant deviation observed between modal frequencies. As part of the FE model calibration, sensitivity analysis is conducted to decrease such deviation. The physical properties selected for the sensitivity analysis are (i) mass density of the concrete and steel, (ii) elastic modulus of the concrete and steel, (iii) translational and rotation stiffness of bearing and soil springs, (ix) moment of inertial of the girder, decking and column sections. The influence curves of each parameter on modal frequencies are plotted. Fig. 5 shows an example of the sensitivity curve of two of the parameters: the elastic modulus of the structural steel $E_{steel}$ and the stiffness of the soil foundation spring $K_{soil}$. It can be observed that $E_{steel}$ has significant effect on dynamic characteristic of the structure, and it is selected as one of the update parameters.

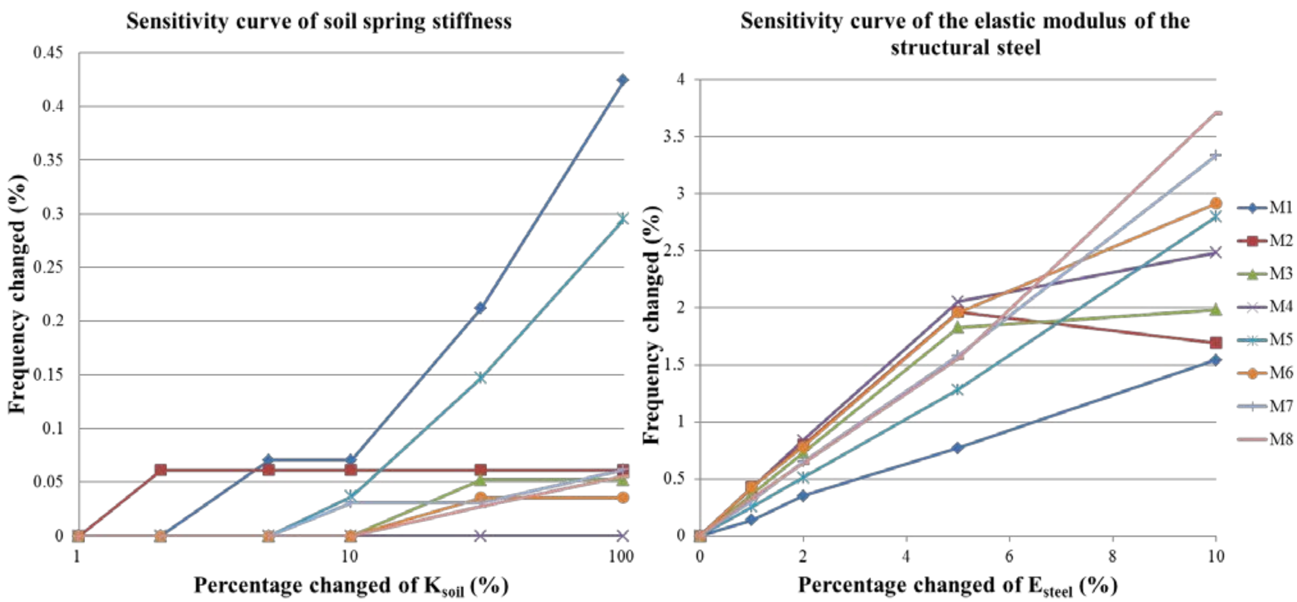


By observing the sensitivity curves, eight parameters were chosen for the FE model optimization. The eight parameters been considered in model updating are: $E_{deck}$, $E_{found}$ and $E_{steel}$ for modulus of elasticity of the decking concrete, foundation concrete and structural steel respectively; $\rho_{deck}$, $\rho_{found}$ and $\rho_{steel}$ for mass density of the three kinds of materials; $K_{U2}$ for translational stiffness of the sliding bearing in bridge longitudinal direction and $I_{col}$ for moment of inertial of the pier column.

## 5. Seismic performance evaluation of the bridge

### 5.1 Performance criteria

In the seismic evaluation of the existing bridges, different performance levels shall be satisfied for different seismic ground motion with a probability of exceedance in 50 years (or different return periods) as specified in Canadian Highway Bridge Design Code 2015. As a Lifeline Bridge, in case of probability of exceedance of 2% in 50 years (return period of 2475 years), the Limited Service level of the service performance levels and the Repairable Performance level of the damage performance levels shall be satisfied. The probability of exceedance of 2% in 50 years was used for the analysis for a more conservative result. The performance criteria for different performance levels are given in CAN/CSA-S6-14 Table 4.16.

### 5.2 Nonlinear hinge model and nonlinear time-history analysis

As specified in CAN/CSA-S6-14 Clause 4.4.6.3, the assessment of damage performance levels shall be carried using nonlinear time-history analysis (NTHA). In order to better represent the actual behavior of the bridge, nonlinear behaviors of certain structural components are incorporated in the model (specifically on the pier columns and cap-beams of the model).

In this study, the nonlinearity of primary components including piers and cap-beams is a major issue in the FE model. As shown in Fig.6, the maximum bending moment will occur at both ends of the column and cap-beam due to lateral load. Therefore, the finite element model assumes that the plastic hinges will form at the critical sections at both ends of the pier columns and cap-beams as shown in Fig.6.

To apply the nonlinear hinge model on the FCB, the moment-curvature diagrams and the P-M interaction curves for each cross-section of columns are calculated. Shear capacity $V_r$ for the primary components (pier columns and cap-beams) are calculated using the following equation:

$$Vr = Vc+Vs$$

$$Vc = 2.5*\beta*\Phi c*fcr*bv*dv \tag{1}$$

$$Vs = \Phi s*fye*Av*dv*\cot\theta \,/\, s$$

where $V_c$ is the shear resistance provided by tensile stresses in concrete, $V_s$ is the shear resistance provided by shear reinforcement. β is the factor used to account for shear resistance of cracked concrete, $f_{cr}$ represents the cracking strength of concrete, $b_V$ and $d_V$ are the effective web width and effective shear depth of section respectively. θ is angle of inclination of the principal diagonal compressive stresses to the longitudinal axis of a member. $A_V$ and s are the area and spacing of transverse reinforcement respectively. The Fiber PMM Hinge model [8] has been applied on all expected location of plastic hinge (which were marked in red circles in Fig. 6).

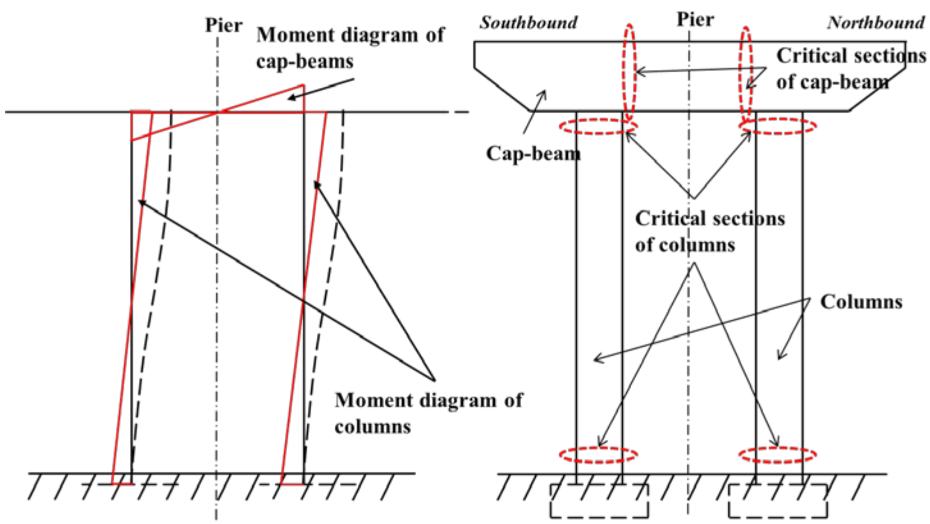


Fig. 6 – Moment diagram of pier under lateral load and expected locations of hinge formation in FCB

## 5.3 Analysis results

Fig.7 shows the axial force at top left section of the Pier No.1 under Cape Mendocino earthquake ground motion. These results are used as seismic demand and are compared with the member capacities to determine the performance criteria. Performance criteria for Limited Service level and Repairable Damage level for seismic evaluation purpose are discussed in the following sections.

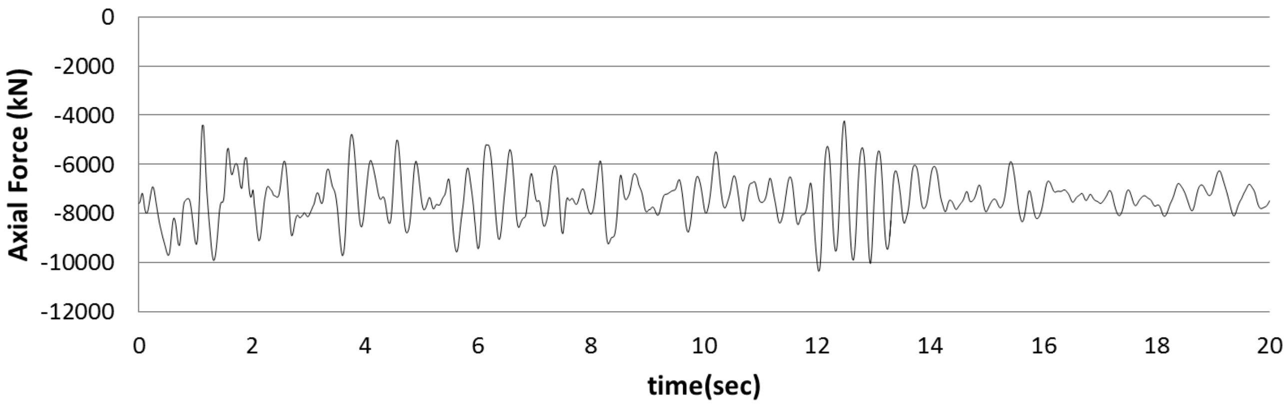


Fig. 7 –Time history record of axial force at top left section of the Pier No.1 (Cape Mendocino)

5.3.1 Concrete structure

The performance criterion requires that reinforcing steel tensile strains shall not exceed 0.015 for concrete component. The axial force and moment calculated for each cross section of each pier is plotted against the P-M target curve, which represents the envelope curve of axial force and moment that produces the maximum reinforcement tensile strength of 0.0015 (Fig. 8). Any data point that may fall outside of that curve will indicate a maximum strain greater than 0.015. It is clearly seen in Fig.8 that all of the data points stays inside the P-M target curve. This proves that the maximum reinforcing steel tensile strains of the columns during nonlinear time history analysis did not exceed 0.015.

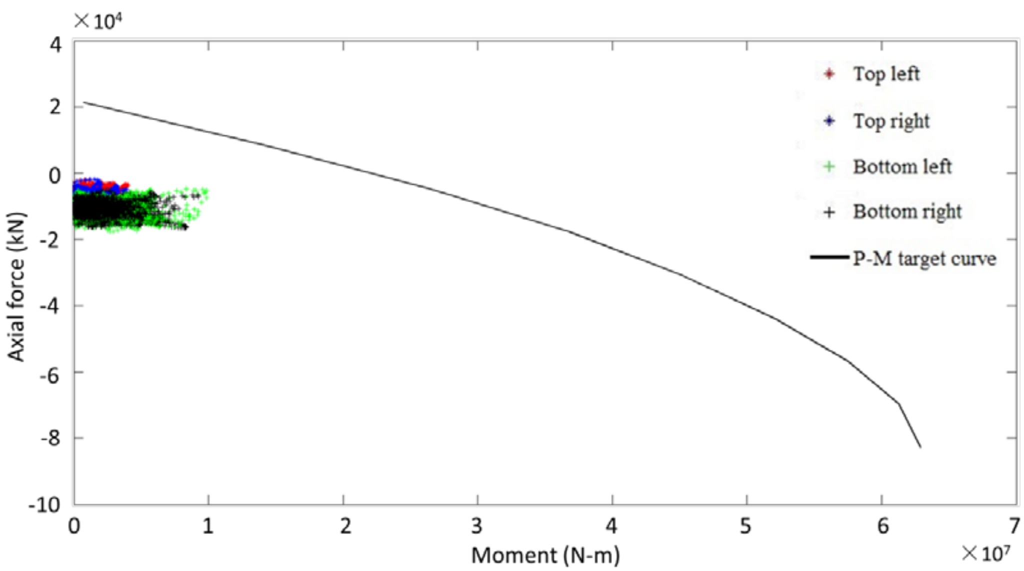


Fig. 8 – Pier column axial-flexural responses compared with P-M performance target curve

For the cap-beams, Table 3 presented the comparison results of bending moment demands with target moments. The target moment was the minimum bending moment that causes the maximum rebar tensile strain of 0.015. The target moment values were calculated as shown in Fig. 56. It can be concluded that the maximum reinforcement strain of the cap-beam did not exceed 0.015, therefore the performance objective is satisfied.

Table 3 – Cap-beam maximum moment compared with target moment

| Section | Max. +Moment (NTHA)(N-m) | Target moment (N-m) |
|---|---|---|
| Capbeam (Pier1) | 7.97E+06 | 3.72E+07 |
| Capbeam (Pier2) | 2.01E+07 | 3.72E+07 |
| Capbeam (Pier3) | 1.81E+07 | 3.72E+07 |

5.3.2 Steel structures (Girders)

The performance criterion requires that no buckling of primary members shall occur. The primary steel members in the bridge are the W-shaped steel girders under the concrete decking. The buckling of steel members was checked by Euler's critical load equation: [9]

$$F = \pi^2 EI/(KL)^2 \tag{2}$$

where F is the expected compressive force on buckling; E is the elastic modulus of the structure steel; I is the moment of inertia of girder section; L is the unsupported length of the element; and K is the effective length factor. However, the top flange all steel girders are rigid connected to the bottom of concrete decking with bolts along the entire length of the steel girder. This makes the unsupported lengths L of the girders equal to zero; therefore, the buckling force of the steel girder will be infinite large. As a result, it can be concluded that the performance requirement of the steel structure was satisfied.

5.3.3 Connections

The primary connections (Fig.6) of the FCB shall not be compromised during the earthquake. In order to verify that the connections were intact, critical beam and column sections of all piers were examined. Both flexural and shear capacities were checked to determine whether there is any possible inelastic behavior which is yielding of the plastic hinge. The flexural capacity was checked as described in performance criteria of concrete structure. Table 4 lists the maximum shear force of columns and the corresponding shear capacity. It can be seen from Table 4 that all column and cap-beam sections are able to withhold the maximum bending moment and shear load. No sign of possible cracking of cover concrete, rebar yielding nor shear failure are found in the NTHA. Therefore, the performance demand related to the connections is satisfied.

5.3.4 Bearings and expansion joints

Elastomeric bearings were allowed to be replaced. The internal shear force in translational directions and the axial force in vertical direction are checked, and the results are summarised in Table 5. The bearing service load capacities are provided in structural drawings. It can be concluded that most service loads of bearing did not meet the maximum force demand; therefore, the bearings of FCB may be damaged during the earthquake and may need to be replaced.

Joints are allowed to be damaged, but they shall be repairable. During the earthquake, the expansion joint located on the bridge will open and close repeatedly in longitudinal direction, possible collision may happen between the concrete decking when the distance come down to zero. In order to find out if the collision happens during time-history analysis, link elements with no stiffness was added between the gaps of expansion joints. By monitoring the deformation of the link element, the maximum values of the relative movement between concrete gaps of the expansion joints can be acquired. The maximum deformation values were summarized from time history analysis results. They were listed and compared with the gap distances of expansion joints in Table 6. It can be concluded that no collision happens during the NTHA

Table 4 Maximum column shear force of time history analysis

| Section location | | | Max. Shear (ETHA)(kN) | Max. Shear (NTHA)(kN) | Shear capacity (kN) |
|---|---|---|---|---|---|
| Pier1 | Top | Left | 14820.00 | 1027.31 | 14820.00 |
| | | Right | 14820.00 | 964.49 | 14820.00 |
| | Bottom | Left | 14820.00 | 1629.08 | 14820.00 |
| | | Right | 14820.00 | 1643.08 | 14820.00 |
| Pier2 | Top | Left | 14820.00 | 1029.28 | 14820.00 |
| | | Right | 14820.00 | 1074.89 | 14820.00 |
| | Bottom | Left | 14820.00 | 2143.42 | 14820.00 |
| | | Right | 14820.00 | 2020.70 | 14820.00 |
| Pier3 | Top | Left | 14820.00 | 1585.83 | 14820.00 |
| | | Right | 14820.00 | 1605.78 | 14820.00 |
| | Bottom | Left | 14820.00 | 2247.96 | 14820.00 |
| | | Right | 14820.00 | 2192.21 | 14820.00 |

Table 5 Bearing maximum shear loads in transverse direction

| Bearing location | Max. Shear (NTHA)(kN) | Shear service loads (kN) |
|---|---|---|
| South pile bent | 1105.12 | 930 |
| Pier 1 | 573.52 | 305 |
| Pier 2 | 1017.96 | 305 |
| Pier 3 (South) | 973.46 | 950 |
| Pier 3 (North) | 902.58 | 295 |
| North abutment | 975.25 | 545 |

Table 6 Maximum expansion joint relative movement of time history analysis

| Joint location | Max. deformation (NTHA) (mm) | Gap distance (mm) |
|---|---|---|
| South pile bent | 23.57 | 300 |
| Pier No.3 | 9.30 | 60 |
| North abutment | 24.76 | 325 |

5.3.5 Displacement

Permanent offset shall not compromise the service and repair requirements of the bridge. No residual settlement or rotation of main structure shall occur. In order to confirm that the bridge meets this demand, the midpoint of the superstructure and the southeast corner of pier foundations were selected as reference points to monitor the residual displacements of the bridge structure. To capture the aftershock behavior, extra time were added at the end of the time history ground motion input. The bridge will continue to vibrate after seismic excitation ends, and vibration amplitude will reduce gradually until it settles at the final residual displacement. The time history results show that no obvious permanent offset or residual displacements occur after the earthquake. Therefore, it can be concluded that the displacement performance criteria are satisfied.

5.3.6 Foundation

Foundation movements shall be limited to only slight misalignment of the spans or settlement of some piers or approaches that does not interfere with normal traffic. To find out the maximum foundation responses at the pier foundations, nodes at southeast corner of the pier foundations were selected as monitored nodes. Peak displacements were summarized in Table 7, which shows that the misalignment or settlements of the foundations under all piers are ignorable. Therefore, it can be concluded that the foundation movement requirement of slight misalignment was satisfied.

Table 7 Maximum pier foundation movements

| Location | Max. UX (NTHA)(mm) | Max. UY (NTHA)(mm) | Max. UZ (NTHA)(mm) |
|---|---|---|---|
| Pier1 | 3.67 | 3.28 | 2.60 |
| Pier2 | 2.36 | 2.43 | 2.80 |
| Pier3 | 2.60 | 4.03 | 3.31 |

## 6. Conclusion

The performance based seismic evaluation procedure was carried out in accordance with the latest Canadian Highway Bridge Design Code 2015. Predetermined capacities of the bridge components have been compared with their demands obtained from nonlinear time history analysis over selected ground motions. For ductile components including all pier columns and cap-beams, the moment and shear capacities both meet the demands. The displacement demands of all expansion joints were satisfied which means no pounding will occur during earthquake. No sign of bucking was noticed for primary steel members. The movements and residual displacements at the superstructure and pier foundations were negligible. The displacement demands on the slide bearings are less than the capacity in longitudinal direction. However, damage form including horizontal shear failure, vertical compressive failure as well as vertical uplift failure may happen on bearings at all five locations. The structural member connected to the bearing was also under high risk of being damaged as well. To sum up, during major earthquake, no primary members will be damaged, the bridge structure should be expected to maintain repairable and operational, and should be capable of supporting the dead load plus full live load after major earthquake. But there is a high possibility that severe damage will happen at all bearings, and structure members connected to the bearing were also subjected to high risk.

## 7. References

[1] Kaya, Y., Ventura, C., Turek, M., & Huffman, S. (2014). British Columbia Smart Infrastructure Monitoring System. In EWSHM-7th European Workshop on Structural Health Monitoring.

[2] Structural Vibration Solutions (SVS) (2001): ARTeMIS Extractor: Ambient Response Testing and Modal Identification Software, User’s Manual.

[3] Computers and Structures Inc. (CSI) (2011): CSIBridge User’s Manual- version 15, Berkeley, California.

[4] Computers and Structures Inc. (CSI) (2011): SAP2000 User's Manual- version 15, Berkeley, California.

[5] Canadian Standards Association. (2015): Canadian highway bridge design code. Canadian Standards Association.

[6] TROMINO User’s Manual, http://www.tromino.eu

[7] Brincker, R., Zhang, L., & Andersen, P. (2001). Modal identification of output-only systems using frequency domain decomposition. Smart materials and structures, 10(3), 441.

[8] Aviram, A., Mackie, K. R., & Stojadinović, B. (2008). Guidelines for nonlinear analysis of bridge structures in California. Pacific Earthquake Engineering Research Center.

[9] Timoshenko, Stephen P., and James M. Gere. (2009) Theory of Elastic Stability. Courier Corporation.